Landscape and Urban Planning 101 (2011) 59–74

Contents lists available at ScienceDirect

Landscape and Urban Planning

journal homepage: www.elsevier.com/locate/landurbplan

Improving the wind environment in high-density cities by understanding urban morphology and surface roughness: A study in Hong Kong

Edward Ng[a,*], Chao Yuan[a], Liang Chen[a], Chao Ren[a], Jimmy C.H. Fung[b,c]

[a] School of Architecture, The Chinese University of Hong Kong, Shatin NT, Hong Kong
[b] Institute for the Environment, The Hong Kong University of Science and Technology, Hong Kong
[c] Department of Mathematics, The Hong Kong University of Science and Technology, Hong Kong

ARTICLE INFO

Article history:
Received 19 August 2010
Received in revised form 6 January 2011
Accepted 10 January 2011

Keywords:
Urban planning
Urban ventilation
Urban roughness
Frontal area density

ABSTRACT

In this study, a high-resolution frontal area density (FAD) map that depicts the surface roughness of urban Hong Kong is produced using a mapping method that takes into account the dense urban morphology and the site wind availability of the territory. Using the MM5/CALMET model simulated wind data of Hong Kong, the FAD map of three urban zones are calculated: podium (0–15 m), building (15–60 m), and urban canopy (0–60 m). The wind tunnel test data is used to correlate the FAD understanding of the three zones. The grid sensitivity test indicates that 200 m × 200 m is the reasonable resolution for the FAD map; the test also establishes that the lower urban podium zone yields the best correlation with the experimental data. The study further establishes that the simpler two-dimensional ground coverage ratio (GCR), which is readily available in the planning circle, can be used to predict the area's average pedestrian level urban ventilation performance of the city. Working with their inhouse GIS team using available data, it allows the planners a way to understand the urban ventilation of the city for decisions related to air paths, urban permeability and site porosity.

© 2011 Elsevier B.V. All rights reserved.

1. Introduction

1.1. Background

Hong Kong has one of the highest densities among mega-cities in the world. Seven and a half million inhabitants live on a group of islands that total 1000 km^2. Hong Kong has a hilly topography; hence, only 25% of the land is built-up areas (Ng, 2009). Land prices in Hong Kong have been increasing over the years. For example, in the Central Business District, rent prices has increased 33% between 2005 and 2007 (HKRVD, 2009). Owing to the limited land area and the increasing land prices, property developers are building taller and bulkier buildings with higher building plot ratios that occupy the entire site area in order to economically cope with the high land costs (Fig. 1). In addition, the Government of Hong Kong has the planned need to deal with an increasing population, which is projected to increase to 10 million in the next 30 years. Seeking ways to optimize the urban morphology of the city is a difficult and important task for urban planners.

Tall and bulky high-rise building blocks with very limited open spaces in between, uniform building heights, and large podium structures have led to lower permeability for urban air ventilation at the pedestrian level (Ng, 2009). The mean wind speeds recorded in urban areas over the last 10 years by the urban observatory stations have decreased by over 40% (HKPD, 2005). Stagnant air in urban areas has caused, among other issues, outdoor urban thermal comfort problems during the hot and humid summer months in Hong Kong. Stagnant air has also worsened urban air pollution by restricting dispersion in street canyon with high building-height-to-street-width ratios. The Hong Kong Environmental Protection Department (EPD) has reported frequent occurrence of high concentrations of pollutants, such as NO_2 and respirable particles (RSP) in urban areas like Mong Kok and Causeway Bay (Yim et al., 2009). These areas have some of the highest urban densities in Hong Kong.

Since the Severe Acute Respiratory Syndrome (SARS) episode in 2003, the planning community in Hong Kong has started to pay more attention to urban design to optimize the benefits of the local wind environment for urban air ventilation. A number of studies have been commissioned by the government. The most important recent project among the government-commissioned studies is entitled "Feasibility Study for Establishment of Air Ventilation Assessment System" (AVA), which began in 2003 (Ng, 2009). The primary purpose of this comprehensive study is to establish the protocol that assesses the effects of major plan-

* Corresponding author. Tel.: +852 2609 6515; fax: +852 2603 5267.
E-mail addresses: edwardng@cuhk.edu.hk (E. Ng), yach@cuhk.edu.hk (C. Yuan), chenliang@cuhk.edu.hk (L. Chen), renchao.cuhk@gmail.com (C. Ren), majfung@ust.hk (J.C.H. Fung).

0169-2046/$ – see front matter © 2011 Elsevier B.V. All rights reserved.
doi:10.1016/j.landurbplan.2011.01.004

Nomenclature

Symbols and abbreviations

A_b	built area in the total lot area (m^2)
A_F	front areas facing the wind direction of θ (m^2)
A_T	total lot area (m^2)
$A(\theta)_{proj(\Delta z)}$	front areas facing the wind direction of θ for a height increment of Δz (m^2)
D	depth of the domain in CFD simulation (m)
L_y	mean breadth of the roughness elements facing the wind direction of θ (m)
GCR	ground coverage ratio (%)
H	height of the domain in CFD simulation (m)
k	coefficient related to GCR and $\lambda_{f(0-15\,m)}$
n	number of buildings
P	annual probability of winds at a particular direction (%)
S_t, S_i	area of wind tunnel tests and area of the grid in the wind tunnel test area (m^2), respectively
V_{-p}	wind speed at the pedestrian level ($m\,s^{-1}$)
V_{-c}	wind speed at the top of urban canopy layer ($m\,s^{-1}$)
$V_{-p,i,j}$	mean wind speed at the pedestrian level at the wind direction of i ($m\,s^{-1}$)
V_{-s}	wind speed at the top of roughness sublayer ($m\,s^{-1}$)
$V_{-z,i}$	mean wind speed at the height of 'z' at the wind direction of i ($m\,s^{-1}$)
$V_{-500,i}$	mean wind speed at 500 m at the wind direction of i ($m\,s^{-1}$)
$VR_{-w,j}$	overall wind velocity ratio
VR_{-500}	average of the directional wind velocity ratios
$VR_{-500,i,j}$	directional wind velocity ratio at the wind direction of i
W	width of the domain in CFD simulation (m)
w	average building width (m)
Δz	height increments in the calculation of $\lambda_{f(z)}$ (m)
zd	zero-plane displacement height (m)
z0	aerodynamic roughness length for momentum (m)
Z_H	mean building height (m)
θ, i	wind direction (°)
α	a power law exponent, which is a constant with the surface roughness, take as 0.35 for this study (urban areas)
$\lambda_{f(\theta)}$	frontal area index at the wind direction of θ
$\lambda_{f(z,\theta)}$	frontal area density at the wind direction of θ
$\lambda_{f(z)}$	frontal area density accounting for the annual wind probability coming from 16 main directions
$\lambda_{f(0-15\,m)}$	frontal area density of the podium layer (Δz: 0–15 m)
$\lambda_{f(15-60\,m)}$	frontal area density of the building layer (Δz: 15–60 m)
$\lambda_{f(0-60\,m)}$	frontal area density of the urban canopy layer (Δz: 0–60 m)
λ_P	plan area fraction
ρ_{el}	density (number) of buildings per unit area
τ_{tp}	pressure drag
τ_{ts}	skin drag

ning and development projects on urban ventilation in Hong Kong (Ng, 2007).

The importance of the wind environment on the physical interaction between urban areas and the atmosphere has been studied by urban climate researchers (Arnfield, 2003). Two kinds of tools are frequently employed to study the wind environment of the city: wind tunnel tests and computational fluid dynamics (CFD) techniques. The US Environmental Protection Agency (EPA) conducted numerous urban-scale wind tunnel tests to understand the dispersion of particulate matters smaller than 10 μm in aerodynamic diameter (PM_{10}) (Ranade et al., 1990). Williams and Wardlaw (1992) conducted a large-scale wind tunnel study to describe the pedestrian-level wind environment in the city of Ottawa, Canada. The study identified areas of concern for planners. Plate (1999) developed the boundary layer wind tunnel studies to analyze urban atmospheric conditions, including wind forces on buildings, pedestrian comfort, and diffusion processes from point-sources of the city. Kastner-Klein et al. (2001) analyzed the interaction between wind turbulence and the effects induced by vehicles moving inside the urban canopy. Wind velocity and turbulence scales throughout the street canyons of the city were analyzed using smoke visualization (Perry et al., 2004). In 2004, the US EPA's Office of Research and Development (EPA-ORD) conducted a city-scale wind tunnel study to analyze the airflow and pollutant dispersion in the Manhattan area (Perry et al., 2004). Kubota et al. (2008) conducted wind tunnel tests and revealed the relationship between plan area fraction (λ_P) and the mean wind-velocity ratio at the pedestrian level in residential neighborhoods of major Japan cities. In Hong Kong, the Wind/Wave Tunnel Facility has conducted numerous tests at the city, district, and urban scale to understand the wind availability and flow characteristics of Hong Kong (HKPD, 2008).

Apart from wind tunnels, CFD model simulation can be helpful at the initial urban planning stage in providing a "qualitative impression" of the wind environment. Mochida et al. (1997) conducted a CFD study to analyze the meso-scale climate in the Greater Tokyo area. Murakami et al. (1999) used CFD simulations to analyze the wind environment at the urban scale. Kondo et al. (2006) used CFD simulations to analyze the diffusion of NO_x at the most polluted roadside areas around the Ikegami-Shinmachi crossroads in Japan. Letzel et al. (2008) conducted studies of urban turbulence characteristics using the urban version of the parallelized Large-eddy Simulation (LES) model (PALM) which is superior to the conventional Reynolds-averaged models (RANS). Using the Earth Simulator, Ashie et al. (2009) conducted the largest urban CFD simulation of Tokyo to understand the effects of building blocks on the thermal environment of Tokyo. Ashie noted that the air temperatures around Ginza and JR Shimbashi are much higher than in the surrounding areas of Hama Park and Sumida River. Ashie argued that the high air temperature can be attributed to the bulky buildings at Ginza and JR Shimbashi that obstruct the incoming sea breezes (Ashie et al., 2009). Yim et al. (2009) used CFD simulation to investigate the air pollution dispersion in a typical Hong Kong urban morphology. In general, using CFD for urban-scale investigation has been gaining momentum in the scientific circle. Recently, two important documents that provide guidelines for CFD usage have been published: AIJ Guidebook (AIJ, 2007; Tominaga et al., 2008) and COST action C14 (Frank, 2006).

1.2. Objectives and needs of this study

The usage of wind tunnels and CFD model simulations to analyze the interaction between the urban area and the atmosphere has made an important contribution to the understanding of urban air ventilation of the city. However, using CFD model simulations and wind tunnel tests in urban planning is expensive. In addition, the CFD model simulations and wind tunnel tests may not be able to keep up with the fast design process in the initial stages of the design and planning decision making process, wherein outlined and district-based information based on urban morphological data parametrically understood can be more useful for planners.

Fig. 1. An urban skyline of Hong Kong.

This paper employs the understanding of urban surface roughness based on the urban structure to establish the relationship between urban morphology and urban air ventilation environment. A new with cross section method is used to calculate the frontal area density (FAD). The terrain in Hong Kong is complicated; hence, the new method also takes into account the site-specific wind rose information at a height of 60 m obtained using the MM5/CALMET model simulation. Using the site-specific wind rose information, the FAD calculation focuses on the effects of the built environment to the wind field. The FAD calculation provides a district-based area average understanding of the wind permeability of the urban area at the urban scale.

The FAD calculation also considers the unique urban morphology of the podiums and towers in Hong Kong. Hong Kong is a high-density city with a unique urban morphology: many tall and slender buildings stand on large podiums. The special morphology of Hong Kong (Fig. 2) shows that taking the urban morphology of podiums into consideration is important; hence, the podium layer is defined within the urban canopy layer. The spatial characteristics of the large podiums reduce the air space nearer to the ground, and can greatly affect the wind environment at the pedestrian level.

This study firstly validates the relationship between the pedestrian-level wind environment and FAD at the podium layer. The study then establishes an understanding of surface roughness and urban morphology based on ground coverage ratio (GCR), a term familiar to urban planners, with FAD to simplify the practical application of the understanding for professional use.

2. Literature review

2.1. Roughness characteristics

The roughness properties of the urban areas affects surface drag, scales and intensity of turbulence, wind speed, and the wind profile in urban areas (Landsberg, 1981). The total drag on a roughness surface includes both a pressure drag (τ_{tp}) on the roughness elements and a skin drag (τ_{ts}) on the underlying surface (Shao and Yang, 2005). In this study, only the pressure drag is considered. This is because the skin drag is relatively small and is not a factor that can be controlled at the urban scale. Oke (1987) provided the logarithmic wind profile in a thermally neutral atmosphere, which is a semi-empirical relationship that acts as a function of two aerodynamic characteristics: roughness length (z0) and the zero-plane displacement height (zd). For setting a base for this logarithmic wind profile that recognized the irregular flow caused by physical bulk in the urban canopy, a new "ground surface" is set (Oke, 2006). As shown in Fig. 2, the height of the new surface is z0 + zd (Oke, 2006). The reliable evaluation of such aerodynamic characteristics of urban areas is significant in depicting and predicting urban wind behaviors (Grimmond and Oke, 1999).

Currently, three classes of methods can be used to estimate the surface roughness: Davenport roughness classification (Davenport et al., 2000), morphometric and micrometeorological methods (Grimmond and Oke, 1999). The Davenport Classification is a surface type classification based on the assorted surface roughness values that use high-quality observations (Davenport et al., 2000). It covers a wide range of surface types. This method is not too help-

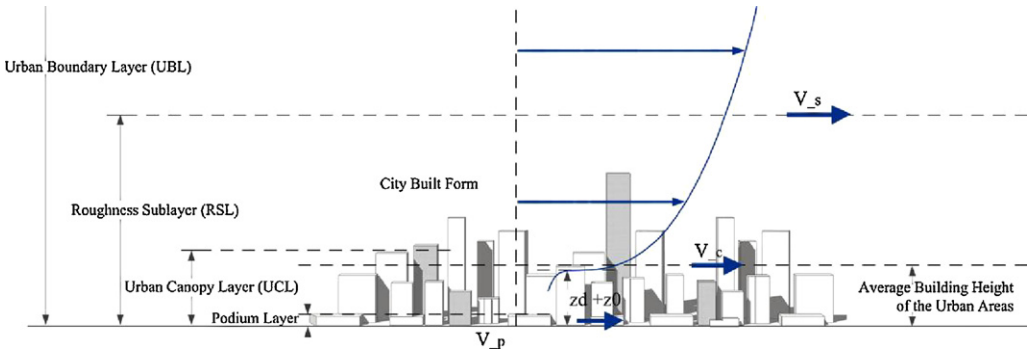

Fig. 2. Wind speed profile, podium layer, urban canopy layer and roughness sublayer. V_{-p}: wind speed at the pedestrian level (2 m above the ground); V_{-c}: wind speed at the top of urban canopy layer; V_{-s}: wind speed at the top of roughness sublayer. The wind speed profile was drawn in accordance with the power law expression: $V_{-z,i}/V_{-500,i} = (Z/500)^{\alpha}$ ($\alpha = 0.35$).

ful to be used to describe urban permeability in high density cities, because most of the urban areas could only be described in Class 8 'Skimming: City centre ($z0 \geq 2$)'. Compared with the micrometeorological method, the morphometric method estimates the aerodynamic characteristics, such as z0 and zd, using empirical equations (Kutzbach, 1961; Lettau, 1969; Raupach, 1992; Bottema, 1996; MacDonald et al., 1998). Grimmond and Oke (1999) validated the empirical models by Kutzbach, Lettau, Raupach, Bottema and Macdonald. Reasonable relationships between z0 and frontal area index ($\lambda_{f(\theta)}$) for low and medium density forms have been found; however, there is a tendency of overestimation of z0 for higher density cases (Bottema, 1996).

Grimmond and Oke (1999) calculated $\lambda_{f(\theta)}$ in the context of the urban morphology of North America cities. Ratti et al. (2002) calculated $\lambda_{f(\theta)}$ of 36 wind directions in London, Toulouse, Berlin, and Salt Lake City. By incorporating a spatially continuous database on aerodynamic and morphometric characteristics, such as $\lambda_{f(\theta)}$, z0 and zd, morphometric estimation methods can be helpful to urban planners and researchers in depicting the distribution of the roughness of the city. Using Bottema's model equation, Gál and Unger (2009) drew a roughness map of z0 and zd to detect the ventilation paths in Szeged. Wong et al. (2010) drew a map of $\lambda_{f(\theta)}$ to detect the air paths in the Kowloon Peninsula of Hong Kong.

2.2. Calculation of frontal area index and frontal area density

The frontal area index $\lambda_{f(\theta)}$ is a function of wind direction of θ, which is an important parameter of the wind environment. The $\lambda_{f(\theta)}$ in a particular wind direction of θ is defined (Raupach, 1992) as

$$\lambda_{f(\theta)} = \frac{A_F}{A_T} = L_y \cdot Z_H \cdot \rho_{el} \quad (1)$$

where A_F represents the front areas of buildings that face the wind direction of θ, A_T represents the total lot area, L_y represents the mean breadth of the roughness elements that face the wind direction of θ, Z_H represents the mean building height, and ρ_{el} represents the density (number) of buildings per unit area. The $\lambda_{f(\theta)}$ has been used widely by researchers in plant canopy and urban canopy communities to help quantify drag force.

Frontal area density, $\lambda_{f(z,\theta)}$, represents the density of $\lambda_{f(\theta)}$ at a height increment of "z" (Burian et al., 2002):

$$\lambda_{f(Z,\theta)} = \frac{A(\theta)_{proj(\Delta z)}}{A_T} \quad (2)$$

where $A(\theta)_{proj(\Delta z)}$ represents the area of building surfaces that approach a wind direction of θ for a specified height increment "Δz" and A_T represents the total lot area of the study area.

Compared with $\lambda_{f(\theta)}$, which is an average value that describes the urban morphology of the entire urban canopy, $\lambda_{f(z,\theta)}$ represents a density that describes the urban morphology in the interested height band. Burian et al. (2002) conducted frontal area density calculations in a height increment of 1 m in Phoenix City, and found that $\lambda_{f(z,\theta)}$ is a function of land uses because the buildings in different land uses have different building morphology. The podium layer and urban canopy layer in Hong Kong have great spatial differences; hence, the use of the respective $\lambda_{f(z,\theta)}$ of the layer is expected to better than $\lambda_{f(\theta)}$ in capturing and describing the complicated urban morphology in Hong Kong.

3. Development of a new method to calculate $\lambda_{f(z)}$ values

Using a high-resolution (1 m × 1 m) three-dimensional building database with building height information and digital elevation model (DEM), a self-developed program embedded as a VBA script in the ArcGIS system is applied to calculate the frontal area density ($\lambda_{f(z)}$) at different height bands. The $\lambda_{f(z)}$ accounts for the annual wind probability from 16 main directions:

$$\lambda_{f(z)} = \sum_{\theta=1}^{16} \lambda_{f(z,\theta)} \cdot P_\theta \quad (3)$$

where $\lambda_{f(z,\theta)}$ represents the frontal area density at a particular wind direction (θ) and can be calculated with Eq. (2). P_θ represents the annual probability of winds at a particular direction (θ).

3.1. Height of the podium and urban canopy layer

To identify the height of the podium and the urban canopy layer in the high-density urban areas of Hong Kong, a statistical study was conducted based on the three-dimensional building database provided by the Hong Kong SAR Government. Twenty five urban areas have been sampled. The mean and upper quartile of the heights of buildings and podiums at the metropolitan and the new town areas were calculated (Fig. 3). According to the distribution (Fig. 4), the heights of the urban canopy layer and podium layer at the metropolitan areas were set at 60 and 15 m, respectively.

As shown in Fig. 5, $\lambda_{f(0-15\,m)}$, $\lambda_{f(15-60\,m)}$, and $\lambda_{f(0-60\,m)}$, representing the podium layer, the building layer, and the urban canopy layer, respectively, were calculated in this study. Their corresponding height increments are 0–15, 15–60, and 0–60 m, respectively.

3.2. Wind of Hong Kong (MM5/CALMET system)

In Hong Kong, the local topography and land-sea contrast causes significant changes in the wind direction in the immediate vicinity of the urban canopy layer (Fig. 5). Therefore, to focus on the drag effect caused by the built environment, the site-specific wind roses for the annual non-typhoon winds at a height of 60 m in 16 directions were used to calculate the corresponding local values of $\lambda_{f(z)}$. Due to the complex topography of Hong Kong and hence the differences in wind roses in different areas, the territory of Hong Kong is divided into sub-areas based on the urban characteristics and the positions of the urban areas for the FAD calculation (Fig. 6). The data on site-specific wind roses were obtained from the fifth-generation NCAR/PSU meso-scale model (MM5) that incorporates the CALMET system (Yim et al., 2007). MM5 is a limited-area, non-hydrostatic, and terrain-following meso-scale meteorological model. MM5 is designed to simulate meso-scale and regional-scale atmospheric circulation (Dudhia, 1993; Yim et al., 2007). CALMET is a diagnostic three-dimensional meteorological model that can interface with MM5 (Scire et al., 2000).

The terrain in Hong Kong is complex; hence, the resolution used in MM5 simulations (typically down to 1 km) cannot accurately capture the effects of the topology characteristics on wind environment. Therefore, CALMET, a prognostic meteorological model capable of higher resolutions (down to 100 m), has been used. Having combined the data obtained using MM5 and the data obtained from an upper air sounding station of the Hong Kong observatory in 2004, the CALMET model adjusts the estimated meteorological fields for the kinematic effects of terrain, slope flows, and terrain blocking effects to reflect the effects of a fine-scale terrain in producing wind fields at 100 m resolutions (Yim et al., 2007). In the CALMET model simulation, the vertical coordinates are set with 10 levels: 10, 30, 60, 120, 230, 450, 800, 1250, 1750, and 2600 m (Yim et al., 2007).

3.3. Calculation of $\lambda_{f(z)}$ in uniform grids

In this study, $\lambda_{f(z)}$ was calculated in uniform grids. Each grid represents a local roughness value. The calculating boundary (grid boundary) is so small that large commercial podiums and public

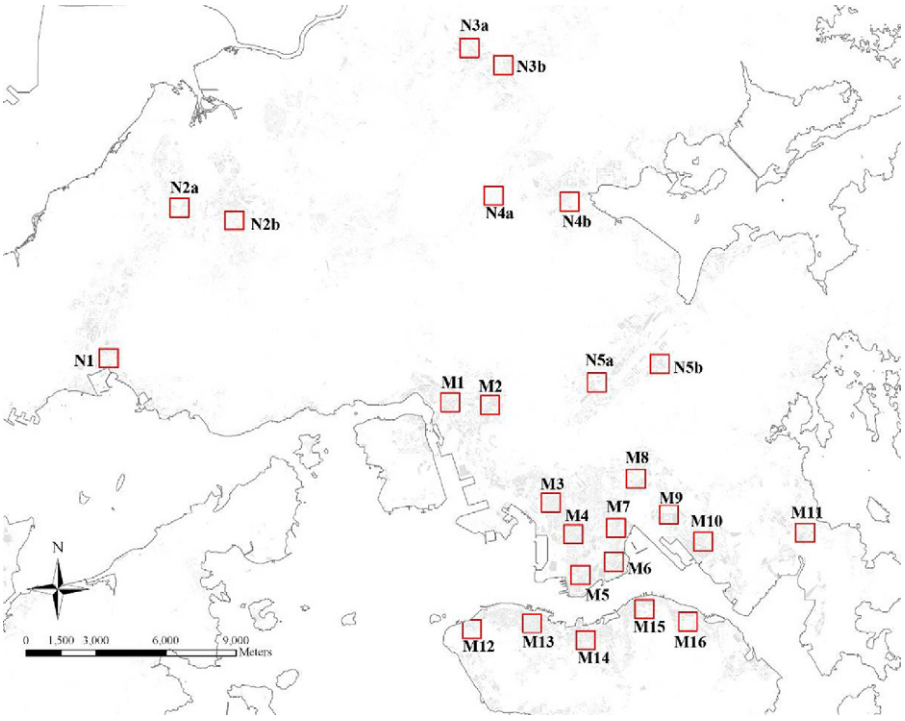

Fig. 3. Twenty five 900 m × 900 m test sites (M: Metropolitan areas; N: New town areas).

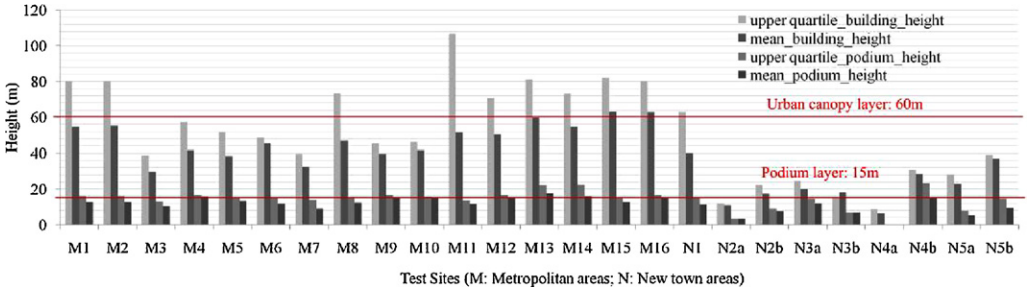

Fig. 4. Heights of the urban canopy layer and the podium layer. Based on the understanding, the heights of the urban canopy layer and the podium layer are set in 60 m and 15 m, respectively, for this study.

transport stations can be larger than the grid cell and cross the grid boundaries (Fig. 7). The value of $\lambda_{f(z)}$ for the cells at the middle of such large buildings may be underestimated. Therefore, to estimate the local roughness of every grid when buildings cross grid cells (Fig. 7), a new method of also accounting for the cross-section areas (red areas) to be included in the frontal areas of the corresponding grid cell is proposed. Compared with the map in polygon units (Gál and Unger, 2009), this new calculation allows an exploration of the uniform grid map with a better explanatory power.

4. Validation of the method and resolution

A statistical study was conducted to validate the FAD calculating method and resolution. Firstly, the cross sections of the new method was validated statistically to the sensitivity of the overall wind velocity ratio ($VR_{-w,i}$), and to the change of the $\lambda_{f(z)}$ calculated with different methods (WITH and No cross sections) in different grid sizes. Secondly, based on the results of the statistical analysis, the resolution was further validated for mapping urban permeability in Hong Kong.

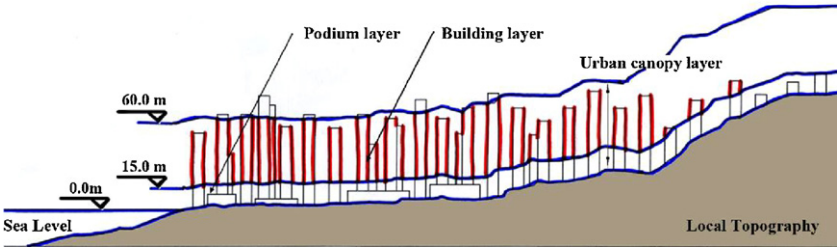

Fig. 5. Illustration of the building layer, podium layer and urban canopy layer.

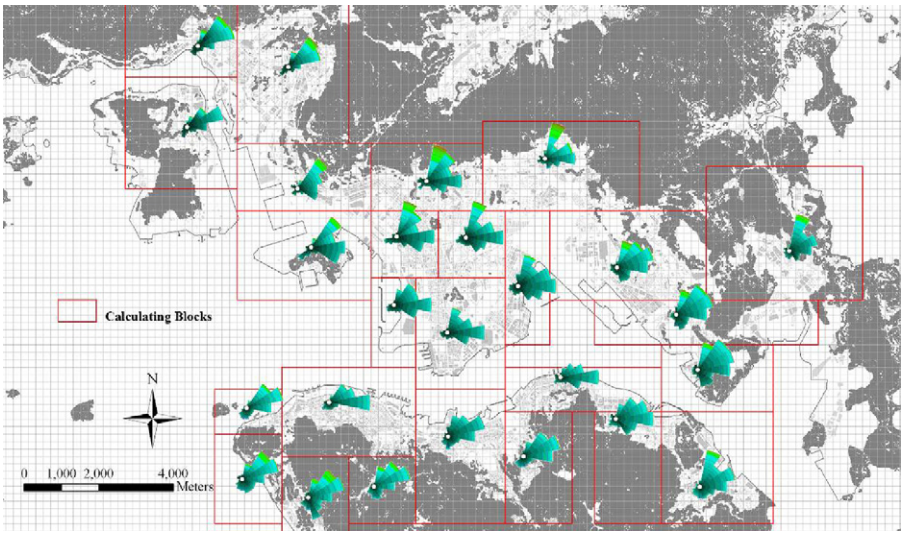

Fig. 6. Calculating blocks and representative wind roses at the height of 60 m in 16 directions for annual non-typhoon winds (01/01/2004–12/30/2004). Data source: (IENV, 2010).

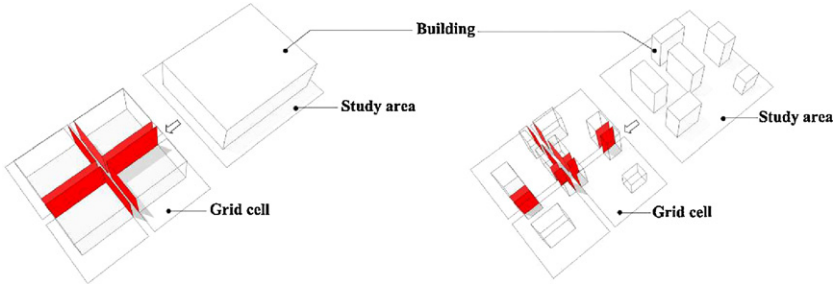

Fig. 7. Cross sections (red area) in two examples. When the study area is uniformly divided into four grid cells, the cross sections are generated. (For interpretation of the references to color in this figure legend, the reader is referred to the web version of the article.)

4.1. Method with cross sections

Based on the more traditional way of calculating FAD, the non-existing walls in the new calculation method could cause the unrealistic surface roughness, however, for high density settings, the cross sections may be needed to avoid the underestimation of the surface roughness at the urban areas covered by large and closely packed buildings. Therefore, the correlations between the $VR_{\_w,i}$ and two methods of $\lambda_{f(z)}$ (WITH and NO cross sections) were compared.

Wind velocity ratios were obtained from wind tunnel tests for Hong Kong (HKPD, 2008). The values of $VR_{\_w,i}$ of 10 study areas in wind tunnel tests were used (Fig. 8). In the wind tunnel tests, test points were uniformly distributed in each of the study areas. The $VR_{\_w,i}$ for each test point is described by (HKPD, 2008):

$$VR_{\_w,j} = \sum_{i=1}^{16} P_i \cdot VR_{\_500,i,j} \tag{4}$$

where P_i represents the annual probability of winds approaching the study area from the wind direction (i), and $VR_{\_500,i,j}$ represents the directional wind velocity ratio of the jth test point, the mean wind speed at 2 m above the ground with respect to the reference at 500 m (HKPD, 2008). $VR_{\_500,i,j}$ is defined as (HKPD, 2008):

$$VR_{\_500,i,j} = \frac{V_{\_p,i,j}}{V_{\_500,i}} \tag{5}$$

where $V_{\_p,i,j}$ represents the mean wind speed of the jth test point at the pedestrian level (2 m above the ground) for wind direction (i), and $V_{\_500,i}$ represents the mean wind speed of the jth test point at 500 m for wind direction (i).

As emphasized in Fig. 9, when the study areas in wind tunnel tests were crossed by grids in the map, the average of $\lambda_{f(z)}$ for the study areas is calculated by

$$\lambda_{f(z)} = \frac{\sum_{i=1}^{4} \lambda_{f\,i(z)} \cdot S_i}{S_t} \tag{6}$$

where $\lambda_{fi(z)}$ represents the frontal area density in the ith grid, S_i represents the area of the ith grid in the study area, and S_t represents the area of the study (Fig. 9).

The $\lambda_{f(z)}$ in the podium layer ($\lambda_{f(0-15\,m)}$) that corresponds to the four grid sizes (resolutions), namely 50, 100, 200, and 300 m, were calculated. The results (R^2) of statistic analysis in Table 1 illustrate that the new calculating method can also accurately predict the wind velocity ratio. As expected and shown in Fig. 10, in accordance with values of the $\lambda_{f(0-15\,m)}$ including the unreal flow-confronting areas are larger than the ones calculated by the more traditional

Table 1
Correlation between $VR_{\_w,j}$ and $\lambda_{f(0-15\,m)}$ in different resolutions and calculation methods.

	R^2 (with cross sections)	R^2 (no cross sections)
Resolution: 300 m × 300 m	0.96	0.96
Resolution: 200 m × 200 m	0.87	0.88
Resolution: 100 m × 100 m	0.71	0.70
Resolution: 50 m × 50 m	0.63	0.66

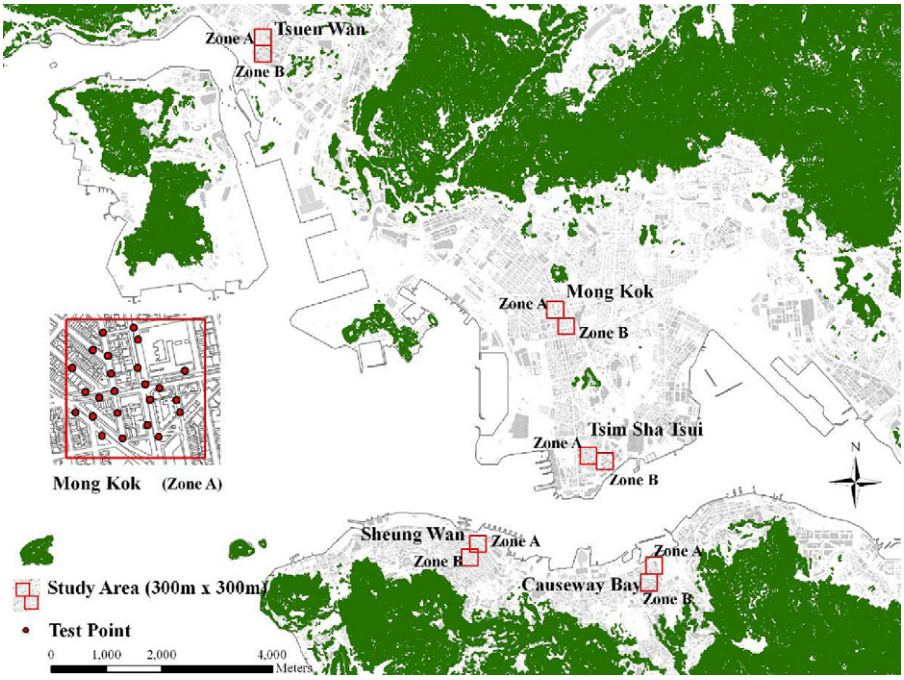

Fig. 8. Wind tunnel study areas in urban areas of Hong Kong.

NO cross section method, and their correlations with VR_{-wj} are similar.

On the other hand, the values of $\lambda_{f(0-15\,m)}$ in the Kowloon Peninsula calculated by the two methods were compared. In high density urban areas with large and closely packed buildings, the values of $\lambda_{f(0-15\,m)}$ calculated by the no cross section method are less than 0.1; some of them are even close to 0. This is a serious underestimation to the surface roughness. Highlighted in Fig. 11, the values by the new method in this study efficiently alleviated these underestimations by including the cross sections.

Based on the validation, the following understanding can be stated: the values of the FAD by the new calculation method with cross sections can correctly predict the wind velocity ratio. Furthermore, compared with the traditional method of calculating the frontal area density, the new method can alleviated the underestimation of mapping urban surface roughness in high density cities with large and closely packed buildings.

4.2. Resolution

As shown in Table 1, the values of R^2 decrease with the reduction of the grid sizes. Choosing a larger grid size would have a positive effect on depicting the urban wind environment. However, R^2 should not be the only criterion for selecting one grid size over

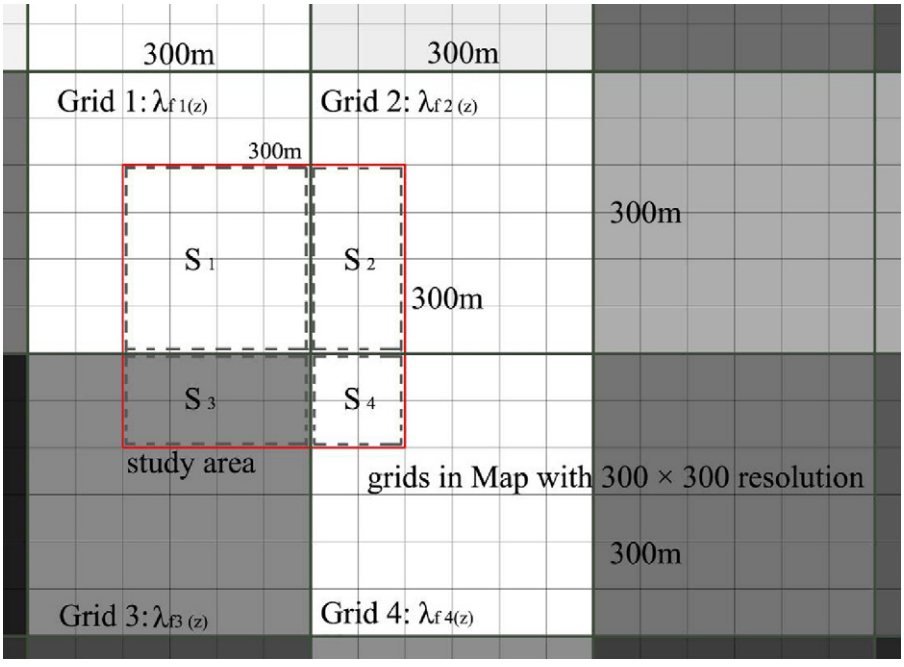

Fig. 9. Calculation of the average of $\lambda_{f(z)}$ in the study area (suppose the resolution is 300 m × 300 m).

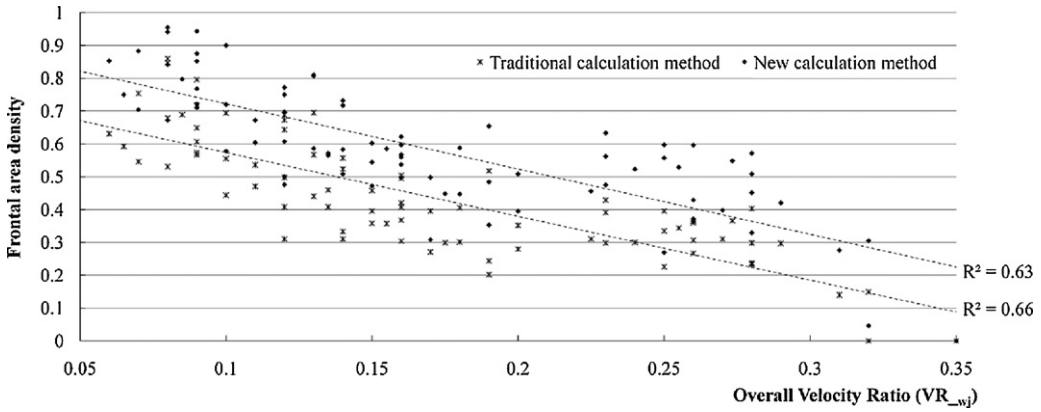

Fig. 10. Relationships between VR_{-wj} and $\lambda_{f(0-15\,m)}$ calculated by different method in 50 m × 50 m resolutions. The number of the point pairs is 80, and the significance level is 5%.

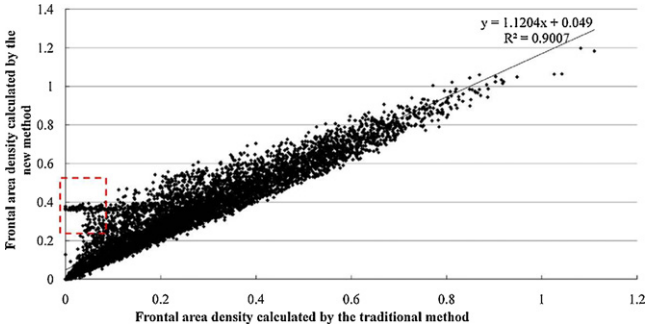

Fig. 11. Relationship between $\lambda_{f(0-15\,m)}$ calculated by different methods in 50 m × 50 m resolutions (test area: Kowloon Peninsula). The number of the point pairs is 7519, and the significance level is 5%.

another. For mapping roughness, the explanatory power of the map should not be totally traded off for the sake of the correctness of $\lambda_{f(z)}$. After weighing the considerations, the resolution of 200 m × 200 m was adopted in mapping urban permeability in Hong Kong.

5. The wind environment and urban morphology at the podium layer

The skimming flow regime is normally found at the top of compact high-rise building areas (Letzel et al., 2008). Similarly, due to the urban morphology of Hong Kong, which is characterized by high density and tall buildings, the airflow above the top of the urban canopy layer may not easily enter into the deep street canyons to benefit the wind environment at the pedestrian level. Thus, the wind velocity ratio at the pedestrian level is mostly dependent on the wind permeability of the podium layer.

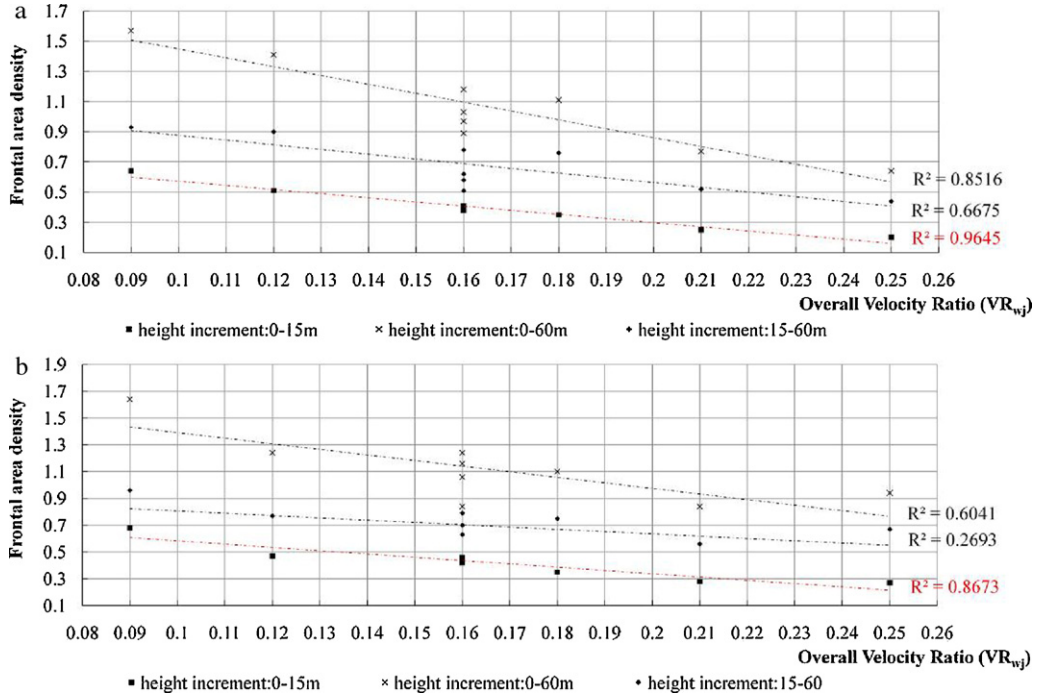

Fig. 12. Relationships between overall velocity ratio (VR_{-wj}) and averaged $\lambda_{f(0-15\,m)}$, $\lambda_{f(15-60\,m)}$ and $\lambda_{f(0-60\,m)}$ in (a) 300 m × 300 m and (b) 200 m × 200 m resolutions. The number of the point pairs is 9, and the significance level is 5%.

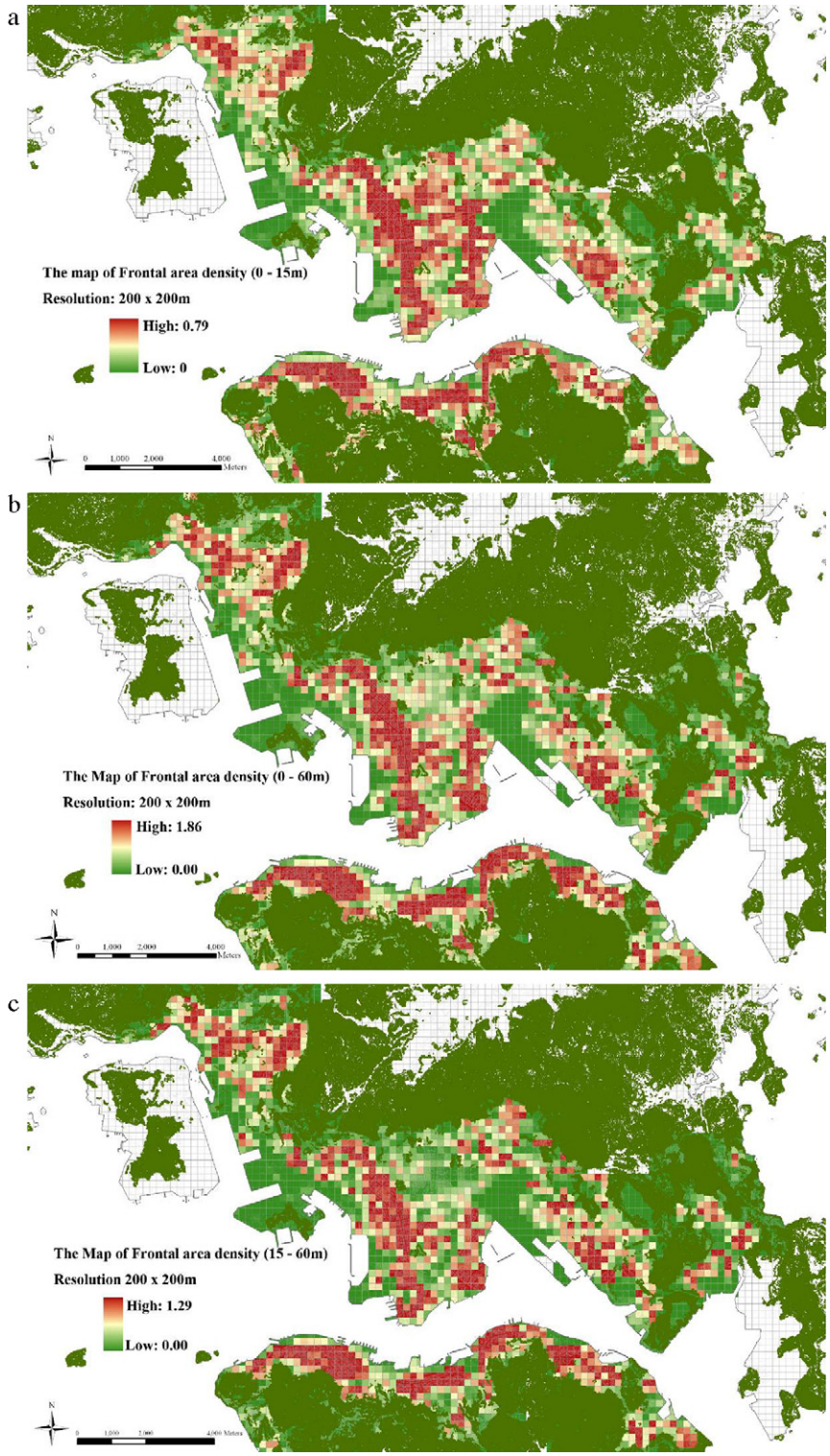

Fig. 13. The map of frontal area density in Kowloon and Hong Kong Island. (a) Resolution: 200 m × 200 m, height increment (Δz): 0–15 m. (b) Resolution: 200 m × 200 m, height increment (Δz): 0–60 m. (c) Resolution: 200 m × 200 m, height increment (Δz): 15–60 m.

A statistical study was conducted to validate the above assumption. This was accomplished by comparing the sensitivities of $VR_{-w,j}$ to changes of $\lambda_{f(z)}$ calculated at different height bands. The results of the validation are plotted in Fig. 12. The values of R^2 in different height bands (Fig. 12a and b) confirm that $VR_{-w,j}$ has a higher correlation with $\lambda_{f(z)}$ at the podium layer (0–15 m). This illustrates that the wind velocity ratio at the pedestrian level is more dependent on the urban morphology at the podium layer (0–15 m) than the building layer (15–60 m) or the whole canopy layer (0–60 m).

This understanding is useful in guiding the urban design and planning strategies toward a quality wind environment at the pedestrian level in high-density urban areas. Compared with front area index, which was used to detect the air paths in Hong

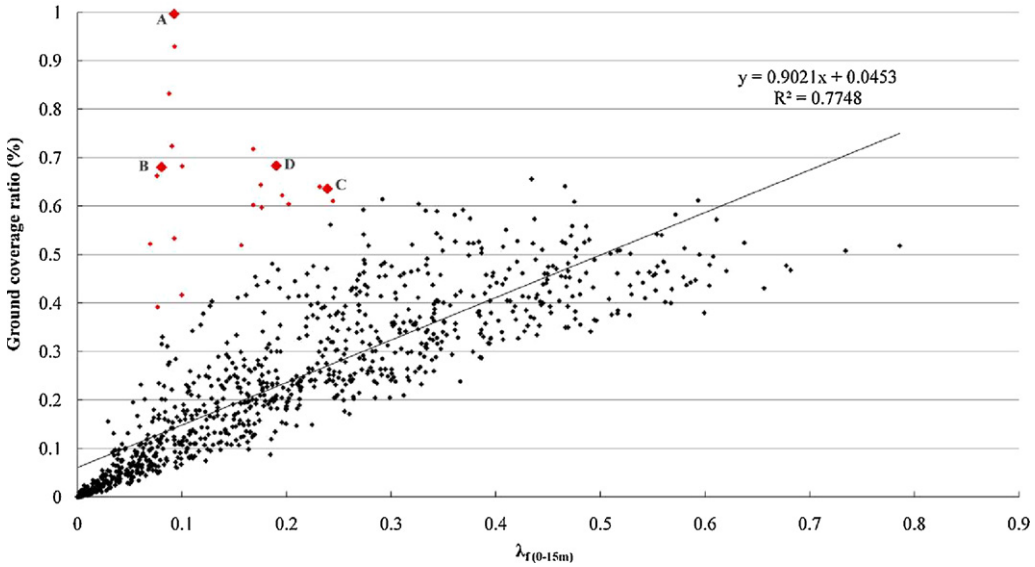

Fig. 14. Relationship between $\lambda_{f(0-15\,m)}$ and GCR in Kowloon Peninsula and Hong Kong Island. The outlier values were highlighted in red. The points A, B, C and D correspond to the four examples in Fig. 16. The number of the point pairs is 1032, and the significance level is 5%. (For interpretation of the references to color in this figure legend, the reader is referred to the web version of the article.)

Kong (Wong et al., 2010), $\lambda_{f(0-15\,m)}$ has been proven to be a better morphological factor in depicting the wind environment at the pedestrian level. The urban morphology at the podium layer decides the wind velocity at the pedestrian level. At the podium level, wind performance mostly depends on the horizontally transport of air. Therefore, high ground-level permeability is conducive to urban ventilation.

As shown in Fig. 13a, the map of the frontal area density (0–15 m) depicts the local wind permeability at the podium layer in the Kowloon Peninsula and Hong Kong Island. The wall effect in the Kowloon Peninsula (Yim et al., 2009) is evident, whereas the wind permeability in most areas of Hong Kong Island, such as the Central District and the Wan Chai, Causeway Bay, is very low. The maps of the frontal area density (0–60 m and 15–60 m) are also presented, as shown in Fig. 13b and c. These two maps are important for describing the wind permeability at the urban canyon layer. The air flow and turbulent mixing at the urban canyon layer are essential for improving urban air ventilation, for alleviating air pollution and for dissipating the anthropogenic heat.

For planners, when referring to Figs. 13a–c, it is important to note the continuous belt of high FAD on the northern coastline of the Hong Kong Island and the two high FAD belts on both sides of the Kowloon peninsula. For mitigating the ill-effects of poorer urban air ventilation, air paths and permeability must be strategically incorporated (Ng, 2009). In Hong Kong, design guidelines of breezeways, air paths and non-building areas have been specified for planners to reference in the Hong Kong Planning Standards and Guidelines (HKPD, 2008).

6. Implementation in urban planning

6.1. Ground coverage ratio and frontal area density

Compared with $\lambda_{f(z)}$, ground coverage ratio (GCR) is a two-dimensional parameter commonly used by architects and urban planners. GCR is defined as

$$\mathrm{GCR} = \frac{A_b}{A_T} = \frac{w^2 \cdot n}{A_T}, \quad (n \geq 1) \tag{7}$$

where A_T represents the domain area, A_b represents the built area, w represents the average building width, and n represents the number of buildings. A statistical study was conducted to convert the analysis in Sections 4 and 5 to a practical design and planning tool; this was accomplished by investigating the relationship between $\lambda_{f(0-15\,m)}$ and GCR.

Local values of $\lambda_{f(0-15\,m)}$ and the GCR of the 1004 test areas (200 m × 200 m) in the Kowloon Peninsula and the Hong Kong Island were calculated. These are the higher density areas in Hong Kong. Fig. 14 shows a good linear correlation of both ($R^2 = 0.77$). However, it should be noted that there are some outlier values of local surface roughness of large podiums and industrial buildings.

To further investigate the reason behind the existence of outliers (Fig. 14), a model was established to conduct a geometric study. Several buildings on a square array created an idealized urban geometry (Fig. 15). The $\lambda_{f(z)}$ can be defined as

$$\lambda_{f(z)} = \frac{\Delta z \cdot w \cdot n}{A_T}, \quad (n \geq 1) \tag{8}$$

where Δz represents the building height increment. Therefore, the relationship between $\lambda_{f(0-15\,m)}$ ($\Delta z = 15$ m) and GCR can be

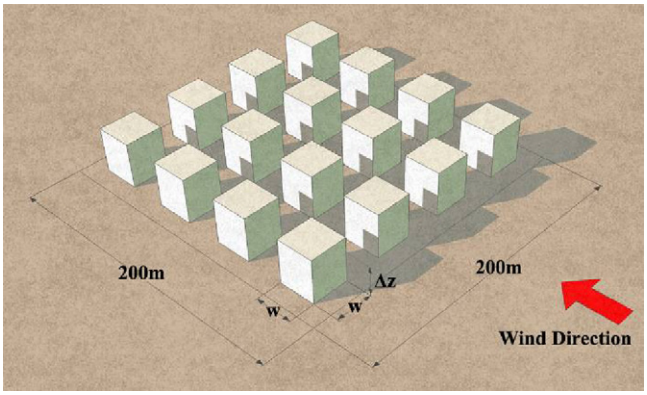

Fig. 15. Idealized urban geometry.

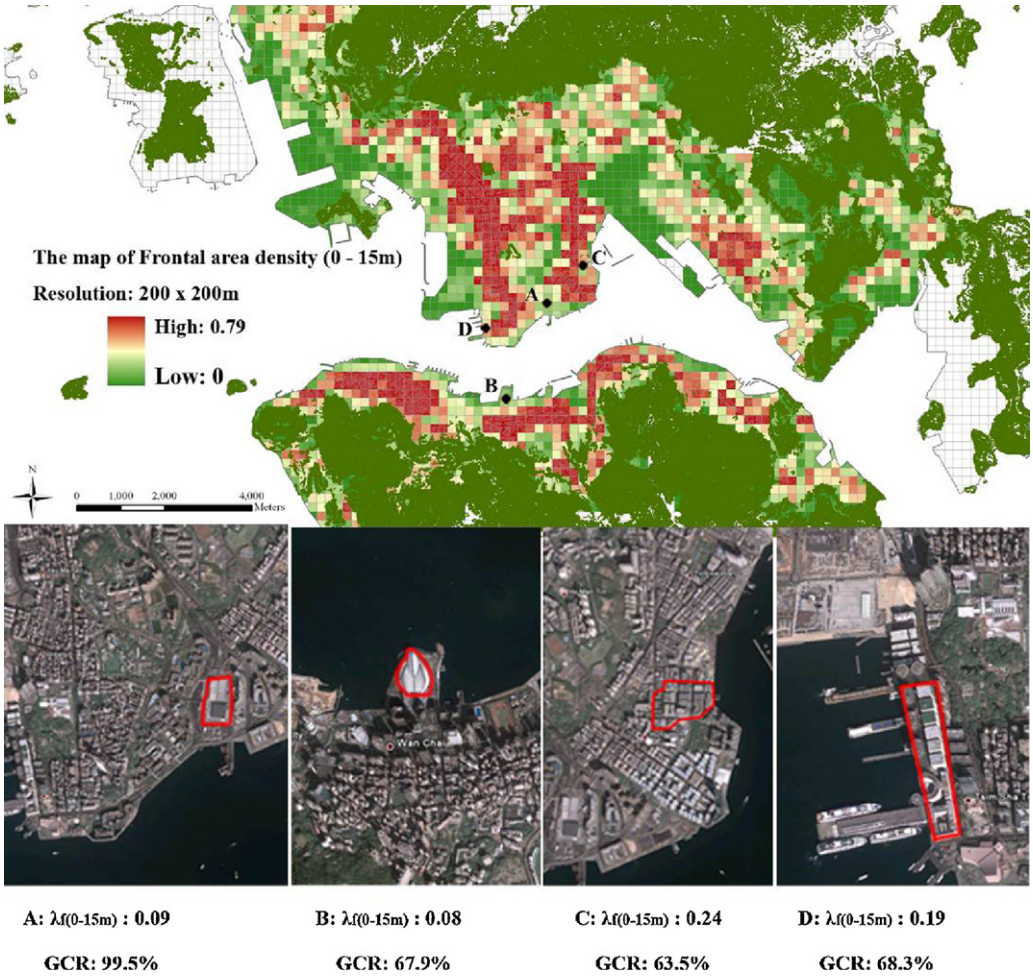

Fig. 16. Four typical cases pointed out in Fig. 14.

expressed by substituting Eq. (8) into Eq. (7)

$$\mathrm{GCR} = \frac{w \cdot \lambda_{f(0-15\,\mathrm{m})}}{15} = k \cdot \lambda_{f(0-15\,\mathrm{m})}, \quad k = \frac{w}{15} \tag{9}$$

where k represents the slope of the linear function. The relationship between $\lambda_{f(z)}$ and GCR clearly depends on the average building width (w). If the building width of urban areas is far larger than that of other areas with normal building morphology, the correlation between GCR and $\lambda_{f(0-15\,\mathrm{m})}$ in such areas can be significantly different from other areas. Four examples of such sites are shown in Figs. 14 and 16.

Having combined Eq. (9), Figs. 14 and 16, the following understanding can be stated:

There is a good linear relationship between $\lambda_{f(0-15\,\mathrm{m})}$ and GCR ($R^2 = 0.77$) in most of the test points. For planners, using GCR to predict the wind environment at the pedestrian level is reasonable. Compared with other maps (Gál and Unger, 2009; Wong et al., 2010), the proposed map is more applicable to urban designers and planners because GCR is one of the most accessible data by planners in the planning process.

Due to the extremely large building widths (large commercial podiums and industrial buildings), local values of some areas may deviate. In this type of sites, the wind permeability cannot be predicted in GCR. However, the occurrence of this type of extreme examples is very small (approximately 2%).

6.2. Mapping the surface roughness (classification)

Based on the analysis in Section 6.1, GCR may be established as an important planning parameter that can be used to describe the wind permeability of the podium layer. An urban-level wind environment map of Hong Kong may be drafted using the GCR information. Kubota et al. (2008) and Yoshie et al. (2008) conducted an earlier investigation on the relationship between GCR and the spatial average of wind velocity ratios at a height of 1.5 m obtained by wind tunnel tests, both in Japanese cities and in the Mong Kok area of Hong Kong. This relationship can be used as the basis for the threshold values of the map classification. Coupled with the classification, the effect of different GCR on the wind permeability can be identified. As shown in Fig. 17, three classification values are assigned: "Class 1," "Class 2," and "Class 3," which denote good, reasonable, and poor pedestrian wind performance, respectively.

Based on this classification, the map of wind performance at the podium layer in Hong Kong was generated (Fig. 18). Compared with the roughness map without classification, the map in this study is more intuitive; in addition, it can aid urban planners better in modifying building morphology to improve the urban air environment. The map can be the spatial reference for urban planners.

After incorporating the respective site-specific wind roses, the areas with low wind permeability are depicted in Fig. 18. These areas block wind and worsen the wind environment at the pedestrian level of their leeward districts. Potential air paths in the podium layer are also marked out in this map. The potential air

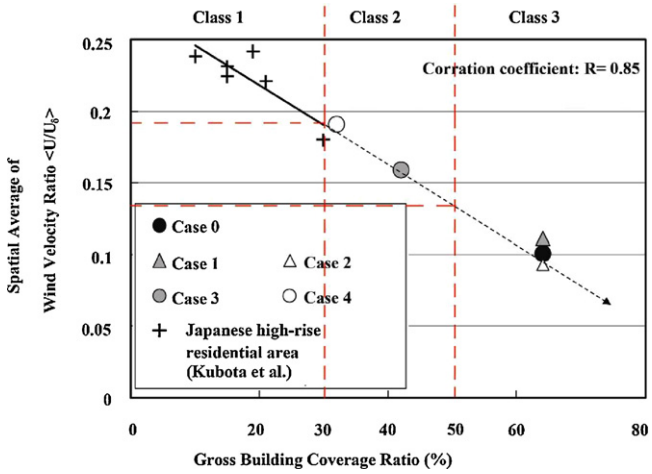

Fig. 17. Relationship between ground coverage ratio and spatial average of wind velocity ratios in Mong Kok and cities in Japan (Kubota et al., 2008; Yoshie et al., 2008, edited by authors). The number of the point pairs is 11.

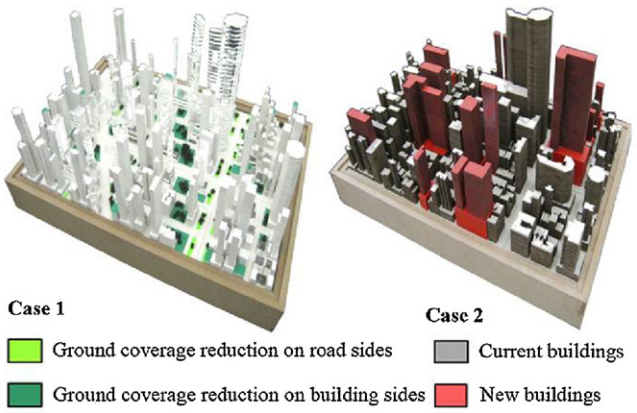

Fig. 19. The case study in Mong Kok, Case 1: the urban design following the understanding in this study; Case 2: the future urban morphology in according with the current planning trend at Mong Kok area.

paths would play an important role to improve the urban ventilation and environment quality by bringing fresh air flow into the urban areas for dissipating air pollutant and for mitigating urban heat island intensity.

7. Case study

As shown in Fig. 18, a case study in a small problematic area, Mong Kok, was conducted to support the analysis in this study. An urban design at this problematic area was produced (Fig. 19, Case 1). For comparison purposes, the future urban morphology, which is in accordance with the current planning trend, was also presented (Fig. 19, Case 2). In this urban design, the urban surface roughness becomes a straightforward design parameter by controlling the GCR. By controlling the GCR (Case 1: 35%; Case 2: 46%), the value of $\lambda_{f(0-15\,m)}$ is decreased from 0.47 in Case 2 to 0.35 in Case 1. This result coincides with the relationship shown in Fig. 14.

A CFD simulation study was conducted to analyze the characteristics of steady-state wind fields in two cases. The κ-ε model was used in CFD numerical algorithms (CFD_Airpak). The domain size was 500 m × 610 m × 260 m [depth (D) × width (W) × height (H)]. In addition, a high grid resolution was applied in this study, that is, the number of fine meshes was approximately 2 million. The surface roughness height was set as 0.3 m, and the inflow boundary condition as set based on the local value of $V_{-500,i}$ (IENV, 2010).

The CFD simulation results (Fig. 20) show that, compared with Case 2, the wind permeability at the entire area is largely optimized in Case 1. As shown in Fig. 21, the frequencies of low wind velocity ratios in Case 1 are lower than that in Case 2. In addition, the frequencies of high wind velocity ratios in Case 1 are higher than that in Case 2. The average of the directional wind velocity ratios (VR_{-500}) is increased from 0.18 in Case 2 to 0.21 in Case 1. This result coincides with the relationship shown in Fig. 17.

The results of this case study prove that, using the urban wind permeability map of the territory (Fig. 18), city planners can easily

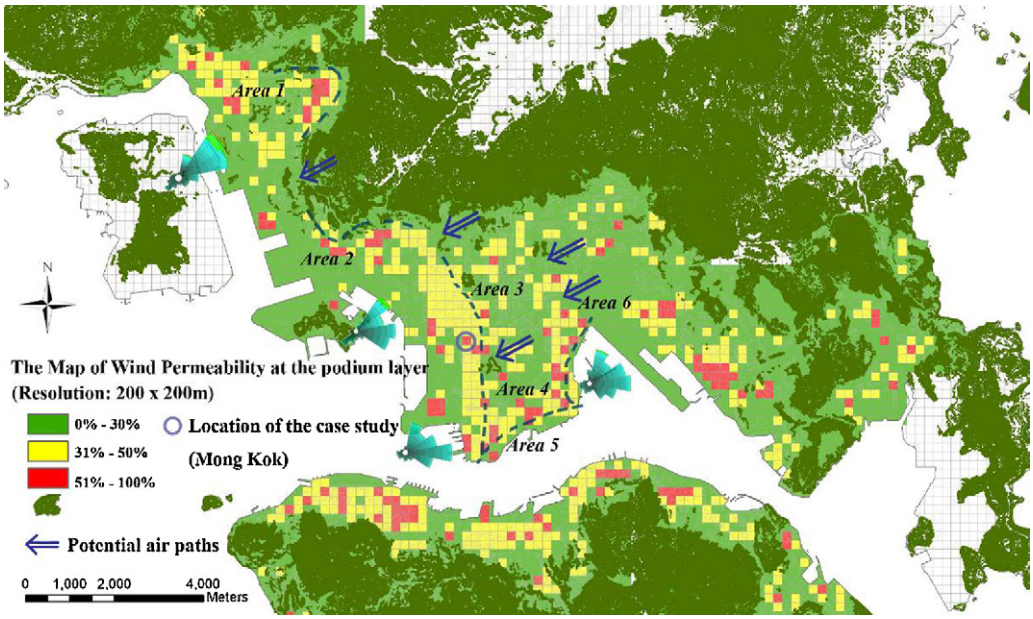

Fig. 18. Map of wind permeability at the podium layer. The wind permeability at the podium level is depicted in the map: Class 1: GCR = 0–30%, Class 2: GCR = 31–50%, Class 3: GCR > 50%. Based on the respective annual prevailing wind direction, the areas with low wind permeability are pointed out. These areas could block the natural ventilation and worse the leeward districts' wind environment at the pedestrian level. Potential air paths in the podium layer are also marked out in this map.

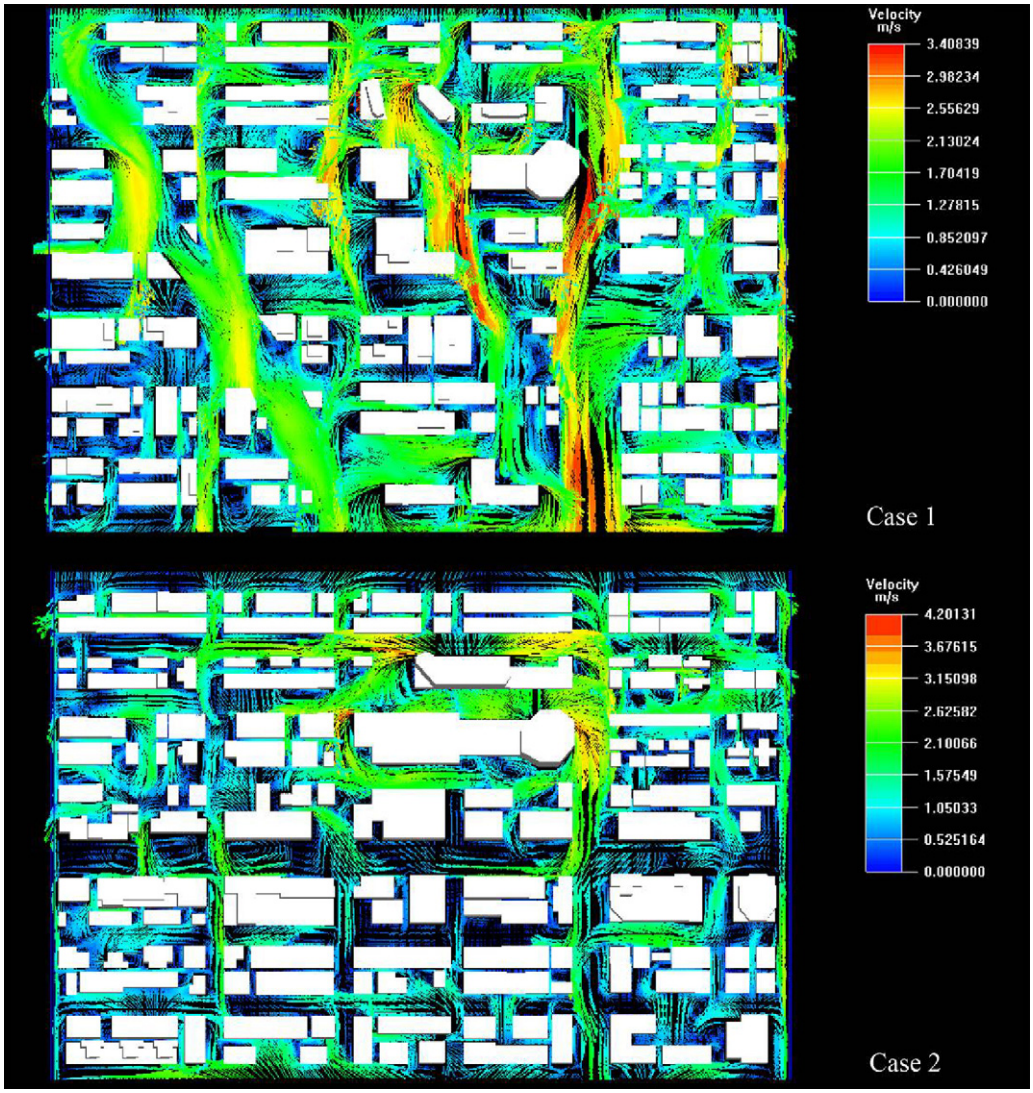

Fig. 20. CFD simulation results: wind environments in Case 1 and Case 2 (2 m above the ground).

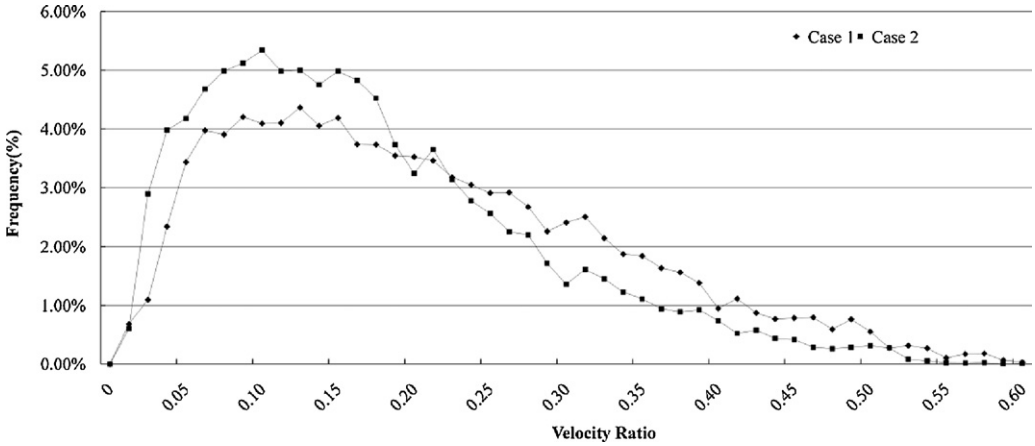

Fig. 21. The frequency of the wind velocity ratios in Case 1 and Case 2.

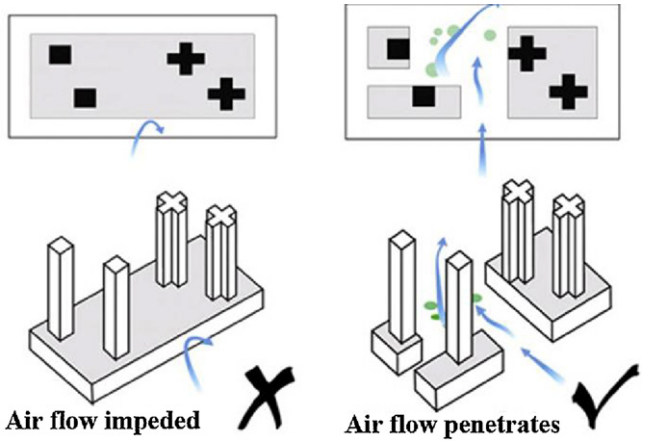

Fig. 22. Podium designs as in the HKPSG.

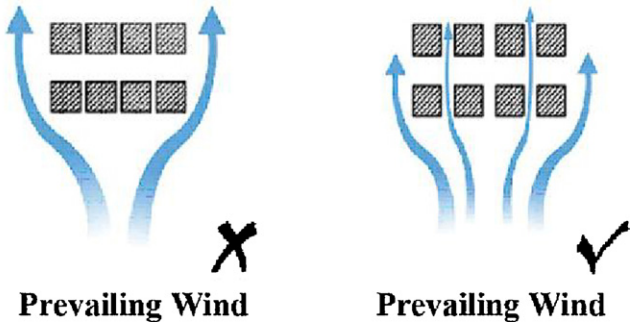

Fig. 24. Building dispositions as in the HKPSG.

detect the problematic areas with poor urban ventilation and optimize them. The understanding in this study can truly improve the urban ventilation at the pedestrian level.

8. Conclusions

The study has highlighted a number of important points that must be considered by city planners. First, one of the most significant factors is urban morphology, especially the podium layer, and its implication to the urban air ventilation environment. According to Chapter 11, Sections 9–13 of the Hong Kong Planning Standards and Guidelines (HKPSG) (HKPD, 2006), a number of urban forms deemed to be conducive to the urban air ventilation environment have been proposed:

> *. . . it is critical to increase the permeability of the urban fabric at the street levels. Compact integrated developments and podium structures with full or large ground coverage on extensive sites typically found in Hong Kong are particularly impeding air movement and should be avoided where practicable. The following measures should be applied at the street level for large development/redevelopment sites particularly in the existing urban areas:*

- *providing setback parallel to the prevailing wind;*
- *designating non-building areas for sub-division of large land parcels;*
- *creating voids in facades facing wind direction; and/or*
- *reducing site coverage of the podia to allow more open space at grade* (Fig. 22)

Where appropriate, a terraced podium design should be adopted to direct downward airflow to the pedestrian level (Fig. 23).

The study shows that the qualitative understanding of the podium structure, as mentioned in the HKPSG, is valid. In Hong Kong, some areas of high podium coverage can be identified. These areas require the most significant design and planning intervention and improvement.

For building block disposition, the study has emphasized that city planners need to factor in the prevailing wind understanding to street layout and building disposition design (Fig. 24). This understanding is in line with the concerns of the so-called "wall buildings," wherein a line of tall buildings screen the waterfront from the inland areas, thereby blocking the incoming urban air ventilation from the sea.

Based on the GCR information readily available to planners working on their GIS system, the study has shown that planners can easily generate an urban wind permeability map of the territory (Fig. 18). This allows the possibility of identifying problem areas and, more importantly, the possibility of emphasizing possible air paths. This also allows the inter-connectivity of open spaces for urban air ventilation, and allows planners to take urban breezeways into account and design in accordance with the recommendations of the HKPSG (HKPD, 2006) (Fig. 25):

> *For better urban air ventilation in a dense, hot-humid city, breezeways along major prevailing wind directions and air paths intersecting the breezeways should be provided in order to allow effective air movements into the urban area to remove heat, gases and particulates and to improve the micro-climate of urban environment.*
>
> *Breezeways should be created in forms of major open ways, such as principal roads, inter-linked open spaces, amenity areas, non-*

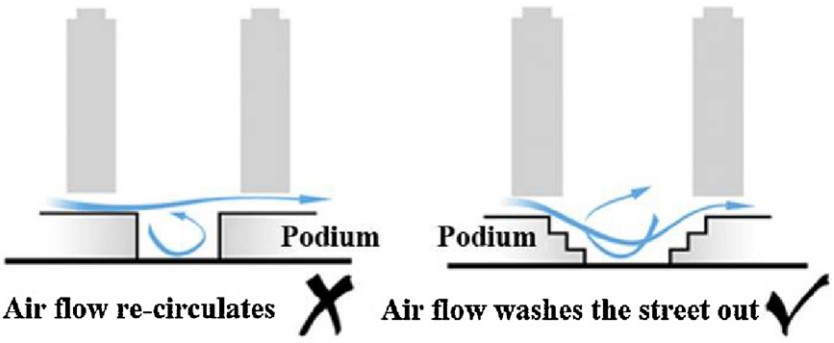

Fig. 23. Terraced podium designs as in the HKPSG.

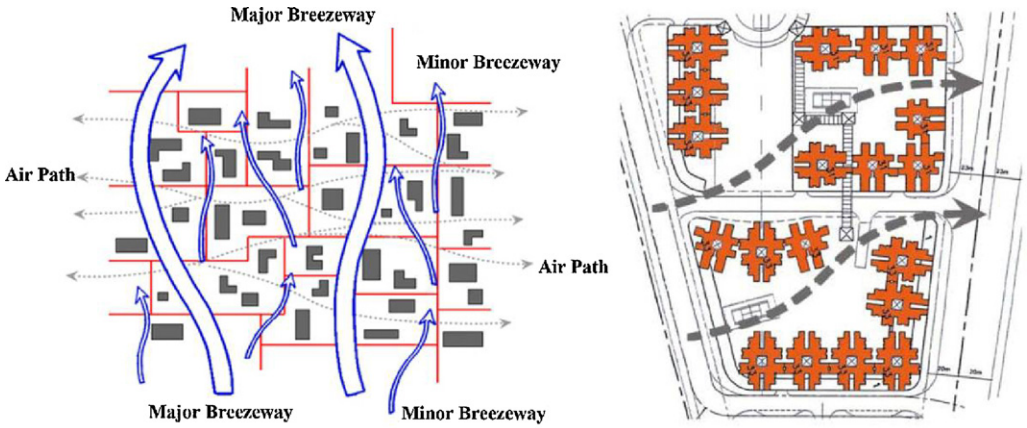

Fig. 25. Breezeway and air path design as in the HKPSG.

building areas, building setbacks and low-rise building corridors, through the high-density/high-rise urban form. They should be aligned primarily along the prevailing wind direction routes, and as far as possible, to also preserve and funnel other natural air flows including sea and land breezes and valley winds, to the developed area.

The disposition of amenity areas, building setbacks and non-building areas should be linked, and widening of the minor roads connecting to major roads should be planned in such a way to form ventilation corridors/air paths to further enhance wind penetration into inner parts of urbanized areas. For effective air dispersal, breezeways and air paths should be perpendicular or at an angle to each other and extend over a sufficiently long distance for continuity.

Using the urban wind permeability map of the territory (Fig. 18), city planners can initially estimate the possible urban air ventilation environment of the urban areas with the average velocity ratios. Adjusting the pedestrian-level wind speeds and predicting the bio-climatic conditions of the city have become possible.

Overall, the study has demonstrated a practical and reliable way for city planners to quickly obtain district-level urban air ventilation information for their board-based design works at the early stages. Conceptually, avoiding wrong decisions that may be difficult to rectify later is therefore possible.

9. Future work

The wind environment in urban areas is complicated. The effects of urban morphological characteristics at the building layer (Fig. 5) to the wind environment can be important. Parametric studies in this layer are necessary.

Acknowledgements

Thanks are due to Professor Jimmy Fung of Hong Kong Science and Technology University (HKUST) for providing the MM5/CALMET data; Planning Department of the Hong Kong SAR Government for providing the planning data; Dr. Peter Hitchcock of HKUST for providing the wind tunnel test data.

References

AIJ (Architectural Institute of Japan), 2007. AIJ Guidebook for Practical Applications of CFD to Pedestrian Wind Environment around Buildings. ISBN 978-4-8189-2665-3.

Arnfield, A.J., 2003. Two decades of urban climate research: a review of turbulence, exchanges of energy and water, and the urban heat island. Int. J. Climatol. 23 (1), 1–26.

Ashie, Y., Hirano, K., Kono, T., 2009. Effects of sea breeze on thermal environment as a measure against Tokyo's urban heat island. In: The Seventh International Conference on Urban Climate , Yokohama, Japan.

Bottema, M., 1996. Roughness parameters over regular rough surfaces: experimental requirements and model validation. J. Wind Eng. Ind. Aerodyn. 64 (2–3), 249–265.

Burian, S.J., Velugubantla, S.P., Brown, M.J., 2002. Morphological Analyses using 3D Building Databases: Phoenix, Arizona. Los Alamos National Laboratory. Available from: <http://www.civil.utah.edu/~burian/Research/ UrbanData/Reports/PHX.pdf>.

Davenport, A.G., Grimmond, C.S.B., Wieringa, T.R.O.J., 2000. Estimating the roughness of cities and sheltered country. In: Proceedings of the 12th Conference on Applied Climatology , Boston.

Dudhia, J., 1993. A nonhydrostatic version of the Penn State-NCAR Mesoscale Model: validation tests and simulation of an Atlantic cyclone and cold front. Mon. Weather Rev. 121, 1493–1513.

Frank, J., 2006. Recommendations of the COST action C14 on the use of CFD in predicting pedestrian wind environment. J. Wind Eng. 108, 529–532.

Gál, T., Unger, J., 2009. Detection of ventilation paths using high-resolution roughness parameter mapping in a large urban area. Build. Environ. 44 (1), 198–206.

Grimmond, C.S.B., Oke, T.R., 1999. Aerodynamic properties of urban areas derived from analysis of surface form. J. Appl. Meteorol. 38, 1262–1292.

HKPD (Hong Kong Planning Department), 2005. Feasibility Study for Establishment of Air Ventilation Assessment System, Final Report. The government of the Hong Kong Special Administrative Region. Available from: <http://www.pland.gov.hk/pland_en/p_study/comp_s/avas/papers&reports/final_report.pdf>.

HKPD (Hong Kong Planning Department), 2006. Hong Kong Planning Standards and Guidelines. The government of the Hong Kong Special Administrative Region. Available from: <www.pland.gov.hk/pland_en/tech_doc/hkpsg/full/ch11/ch11_text.htm>.

HKPD (Hong Kong Planning Department), 2008. Urban Climatic Map and Standards for Wind Environment – Feasibility Study, Working Paper 2B: Wind Tunnel Benchmarking Studies, Batch I. The government of the Hong Kong Special Administrative Region. Available from: <http://www.pland.gov.hk/pland_en/p_study/prog_s/ucmapweb/ucmap_project/content/reports/wp2b.pdf>.

HKRVD (Hong Kong Rating and Valuation Department), 2009. Private Office – 1984–2007 Rental and Price Indices for Grade A Office in Core Districts. The government of the Hong Kong Special Administrative Region. Available from: <http://www.rvd.gov.hk/en/doc/statistics/his_data_10.pdf>.

IENV (Institute for the Environment), 2010. Study of Ventilation over Hong Kong. The Hong Kong University of Science and Technology. Available from: <http://envf.ust.hk/vent/>.

Kastner-Klein, P., Fedorovich, E., Rotach, M.W., 2001. A wind tunnel study of organised and turbulent air motions in urban street canyons. J. Wind Eng. Ind. Aerodyn. 89 (9), 849–861.

Kondo, H., Asahi, K., Tomizuka, T., Suzuki, M., 2006. Numerical analysis of diffusion around a suspended expressway by a multi-scale CFD model. Atmos. Environ. 40 (16), 2852–2859.

Kubota, T., Miura, M., Tominaga, Y., Mochida, A., 2008. Wind tunnel tests on the relationship between building density and pedestrian-level wind velocity: development of guidelines for realizing acceptable wind environment in residential neighborhoods. Build. Environ. 43 (10), 1699–1708.

Kutzbach, J., 1961. Investigations of the modifications of wind profiles by artificially controlled surface roughness. Department of Meteorology, University of Wisconsin-Madison, M.S. thesis.

Landsberg, H.E., 1981. The Urban Climate. Academic Press, Inc. (London) Ltd., London.

Lettau, H., 1969. Note on aerodynamic roughness-parameter estimation on the basis of roughness-element description. J. Appl. Meteorol. 8, 828–832.

Letzel, M.O., Krane, M., Raasch, S., 2008. High resolution urban large-eddy simulation studies from street canyon to neighbourhood scale. Atmos. Environ. 42 (38), 8770–8784.

MacDonald, R.W., Griffiths, R.F., Hall, D.J., 1998. An improved method for the estimation of surface roughness of obstacle arrays. Atmos. Environ. 32 (11), 1857–1864.
Mochida, A., Murakami, S., Ojima, T., Kim, S., Ooka, R., Sugiyama, H., 1997. CFD analysis of mesoscale climate in the Greater Tokyo area. J. Wind Eng. Ind. Aerodyn. 67–68, 459–477.
Murakami, S., Ooka, R., Mochida, A., Yoshida, S., Kim, S., 1999. CFD analysis of wind climate from human scale to urban scale. J. Wind Eng. Ind. Aerodyn. 81 (1–3), 57–81.
Ng, E., 2007. Feasibility study for establishment of air ventilation assessment system (AVAS). J. HKIP 22 (1), 39–45.
Ng, E., 2009. Policies and technical guidelines for urban planning of high-density cities – air ventilation assessment (AVA) of Hong Kong. Build. Environ. 44 (7), 1478–1488.
Oke, T.R., 1987. Boundary Layer Climates. Methuen, Inc., USA.
Oke, T.R., 2006. Initial guidance to obtain representative meteorological observations at urban sites. WMO/TD No. 1250, pp. 21–22.
Perry, S.G., Heist, D.K., Thompson, R.S., Snyder, W.H., Lawson, R.E., 2004. Wind tunnel simulation of flow and pollutant dispersal around the World Trade Centre site. Environ. Manager, 31–34.
Plate, E.J., 1999. Methods of investigating urban wind fields-physical models. Atmos. Environ. 33 (24–25), 3981–3989.
Ranade, M.B., Woods, M.C., Chen, F.L., Purdue, L.J., Rehme, K.A., 1990. Wind tunnel evaluation of PM10 samplers. Aerosol Sci. Technol. 13 (1), 54–71.
Ratti, C., Sabatino, S.D., Britter, R., Brown, M., Caton, F., Burian, S., 2002. Analysis of 3-D urban databases with respect to pollution dispersion for a number of European and American cities. Water Air Soil Pollut.: Focus 2, 459–469.
Raupach, M.R., 1992. Drag and drag partition on rough surfaces. Bound.-Lay. Meteorol. 60, 375–395.
Scire, J.S., Robe, F.R., Fernau, M.E., Yamartino, R.J., 2000. A User's Guide for the CALMET Meteorological Model (Version 5). Earth Tech, Inc. Available from: http://www.src.com/calpuff/download/CALMET_UsersGuide.pdf.
Shao, Y., Yang, Y., 2005. A scheme for drag partition over rough surfaces. Atmos. Environ. 39 (38), 7351–7361.
Tominaga, Y., Mochida, A., Yoshie, R., Kataoka, H., Nozu, T., Yoshikawa, M., Shirasawa, T., 2008. AIJ guidelines for practical applications of CFD to pedestrian wind environment around buildings. J. Wind Eng. Ind. Aerodyn. 96, 1749–1761.
Williams, C.D., Wardlaw, R.L., 1992. Determination of the pedestrian wind environment in the city of Ottawa using wind tunnel and field measurements. J. Wind Eng. Ind. Aerodyn. 41 (1–3), 255–266.
Wong, M.S., Nichol, J.E., To, P.H., Wang, J., 2010. A simple method for designation of urban ventilation corridors and its application to urban heat island analysis. Build. Environ. 45 (8), 1880–1889.
Yim, S.H.L., Fung, J.C.H., Lau, A.K.H., Kot, S.C., 2007. Developing a high-resolution wind map for a complex terrain with a coupled MM5/CALMET system. J. Geophys. Res. 112, D05106.
Yim, S.H.L., Fung, J.C.H., Lau, A.K.H., Kot, S.C., 2009. Air ventilation impacts of the "wall effect" resulting from the alignment of high-rise buildings. Atmos. Environ. 43 (32), 4982–4994.
Yoshie, R., Tanaka, H., Shirasawa, T., Kobayashi, T., 2008. 香港の高層密集市街地における風通しに関する研究：その 1 建蔽率と建物高さのバリエーション等が歩行者レベルの風速・気温分布に及ぼす影響 (Experimental study on air ventilation in a built-up area with closely-packed high-rise building). J. Environ. Eng. 627, 661–667 (in Japanese).